Staufenbiel, S.; Merino, M.; Li, W.; Huang, M.-D.; Baudis, S.; Lendlein, A.; Mueller, R.H.; Wischke, C.:

**Surface characterization and protein interaction of a series of model poly[acrylonitrile-co-(N-vinyl pyrrolidone)] nanocarriers for drug targeting**

In: International Journal of Pharmaceutics (2015) Elsevier

DOI: 10.1016/j.ijpharm.2015.02.072

# Surface characterization and protein interaction of a series of model poly[acrylonitrile-*co*-(*N*-vinyl pyrrolidone)] nanocarriers for drug targeting

Sven Staufenbiel [1,2], Marian Merino [1,3], Wenzhong Li [3], Mao-Dong Huang [4], Stefan Baudis [3], Andreas Lendlein [1,3], Rainer H. Müller[1,2], Christian Wischke [1,3] *

[1] Helmholtz Virtual Institute for Multifunctional Biomaterials for Medicine, Teltow, Germany

[2] Institute of Pharmacy, Freie Universität Berlin, Kelchstr. 31, 12169 Berlin, Germany

[3] Institute of Biomaterial Science and Berlin-Brandenburg Center for Regenerative Therapies, Helmholtz-Zentrum Geesthacht, Kantstr. 55, 14513 Teltow, Germany

[4] Leibniz-Institut für Analytische Wissenschaften (ISAS), Schwarzschildstr. 8, 12489 Berlin, Germany

* Corresponding author: Christian.Wischke@hzg.de, Tel. +49 (0) 3328 352-450, Fax +49 (0) 3328 352-452; Institute of Biomaterial Science and Berlin-Brandenburg Center for Regenerative Therapies, Helmholtz-Zentrum Geesthacht, Kantstr. 55, 14513 Teltow, Germany

## Abstract

The surface properties of intravenously injected nanoparticles determine the acquired blood protein adsorption pattern and subsequently the organ distribution and cellular recognition. A series of poly[acrylonitrile-*co*-(*N*-vinyl pyrrolidone)] (PAN) model nanoparticles (133-181 nm) was synthesized, in which the surface properties were altered by changing the molar content of NVP (0 to 33.8 mol-%) as the more hydrophilic repeating unit. The extent of achieved surface property variation was comprehensively characterized. The residual sodium dodecyl sulfate (SDS) content from the synthesis was in the range 0.3-1.6 $\mu g \cdot ml^{-1}$, potentially contributing to the surface properties. Surface hydrophobicity was determined by Rose Bengal dye adsorption, hydrophobic interaction chromatography (HIC) and aqueous two-phase partitioning (TPP). Particle charge was quantified by zeta potential (ZP) measurements including ZP-pH profiles. The interaction with proteins was analyzed by ZP measurements in serum and by adsorption studies with single proteins. Compared to hydrophobic polystyrene model nanoparticles, all PAN were very hydrophilic. Differences in

surface hydrophobicity could be detected, which did not linearly correlate with the systematically altered bulk composition of the PAN nanoparticles. This proves the high importance of a thorough surface characterization applying a full spectrum of methods, complementing predictions solely based on bulk polymer composition.

Keywords:

Polymer nanoparticles, protein adsorption, surface characterization, poly[acrylonitrile-*co*-(*N*-vinyl pyrrolidone), surface hydrophobicity, targeting

## 1. Introduction

The still unrealized pharmaceutical dream is to design intravenously administered nanocarriers for site specific targeting in a controlled way *in vitro*. Trial and error should be replaced by controlled development. The meanwhile accepted theory for achieving this aim is the theory of differential protein adsorption: intravenously injected particles adsorb a distinct pattern of proteins, which then defines their *in vivo* fate, e.g. rapid uptake by the immune system (mainly liver and spleen macrophages), long-term circulation in the blood stream, or accumulation in specific tissues (e.g. brain, bone marrow). The composition of the protein corona bound to the polymeric nanocarriers is determined by the physico-chemical properties of the nanocarrier surface, e.g. charge, surface hydrophobicity, functional groups etc. Knowing this correlation of “surface properties − adsorption pattern − organ distribution”, one can theoretically design nanocarriers with surface properties, which lead automatically to a preferential adsorption of proteins that mediate the adherence to the desired target area (Müller and Heinemann, 1989).

The principal capability of a differential protein adsorption mediating organ distribution has been realized by chance in very few cases. One of the most prominent examples are Tween® 80-coated polymeric nanoparticles loaded with darlagin (Kreuter et al., 1997). After injection, they preferentially adsorb apolipoprotein E leading to uptake and penetration across the

blood-brain barrier (Müller, 2001). Still, this carrier concept is not yet perfect. As for most nanocarriers dedicated for a distinct organ targeting, there is a competitive accumulation in other tissues, in this case in the liver, which leads to only a minor fraction localizing in the brain. However, these particles prove that the approach of differential adsorption is working in principle. To develop nanocarriers in a controlled way, one needs to thoroughly analyze their physicochemical properties with relevance for the protein adsorption pattern and organ distribution.

Many studies are limited to the characterization of only two nanoparticle properties (e.g. typically size and charge), which is not sufficient to fully understand relevant aspects such as surface hydrophobicity that are often completely neglected. More systematic characterization studies have been performed with non-biodegradable surface modified polystyrene model nanoparticles (Armstrong et al., 1997; Gessner et al., 2002; Gessner et al., 2003; Moghimi, 1997, 2002; Moghimi et al., 1993; Nagayama et al., 2007; Ogawara et al., 2004). It should be noted that hydrophobicity is often not experimentally assessed but hypothesized from the chemical nature of the matrix material of the particle. However, surface properties are not only defined by the matrix (bulk) composition, but are influenced by many other factors such as preferential orientation of polymer segments in the interphase, the distribution of the comonomers in the polymer chains, the presence of surfactants used for stabilizing nascent particles during preparation, or chemical alteration of moieties exposed at the surface. Importantly, besides specific functional ligands causing selective protein binding, surface hydrophobicity is a key parameter for the adsorption of blood proteins and should be quantified by analytical methods in addition to assumptions based on the bulk polymer composition.

Ideally, the applied methods should yield data having relevance for the *in vivo* situation. One occasionally followed approach is the characterization of contact angles of compressed dry nanoparticle films; however, these data may not be predictive as the nanoparticles are not analyzed in their original aqueous environment, i.e. in the hydrated state, but require intermediate drying steps. Alternatively, nanocarriers may be studied in their original

aqueous suspension by standardized adsorption of detectable probes such as dyes or by a comparative analysis of nanoparticle retention at stationary phases with different surface functionalization.

To move away from polystyrene and to put the analysis on a broader basis, a series of poly[acrylonitrile-*co*-(*N*-vinyl pyrrolidone)] [PAN] nanoparticles with systematic variation of their composition based on acrylonitrile (AN) and *N*-vinyl pyrrolidone (NVP) as co-monomers should be analyzed (Li et al., 2012). While polyacrylonitrile is a water-insoluble polymer, poly(*N*-vinyl pyrrolidone) [PVP] is water soluble, thus more hydrophilic. These materials are generally considered to be non-degradable and thus are suitable as model systems that do not experience substantial alteration of properties in aqueous environment, although it cannot be absolutely excluded that exposed moieties at the surface may to a minor extent be subject of a chemical alteration like hydrolysis. Such nanoparticles, in this case with a fluorescent dye loading, illustrated a very rapid dose-dependent endocytosis by endothelial cells *in vitro* in serum-based cell culture medium for nanoparticles with low NVP content. In contrast, nanoparticles with an NVP content ≥ 20 mol-% were incorporated only by a small fraction of the cells, which was not systematically enhanced when strongly increasing the particle dose (Wischke et al., 2013).

Apparently, a variation in the copolymer composition of PAN can result in differences in biological recognition and subsequent cellular fate. However, it remains to be shown to which extent the surface properties of the nanoparticles as well as the protein interaction differ within this family of materials and can account for the observed biological effect. Nanoparticles with “theoretically predicted” different hydrophobicity were synthesized by miniemulsion polymerization with variation of the NVP content between 0 and 33.8 mol-%. Since miniemulsion polymerization requires the use of a detergent such as sodium dodecyl sulfate (SDS) that subsequently is removed by dialysis to the greatest possible extent, the analysis of residual surfactant was included. Accordingly, in this study, the model nanocarriers were intensively characterized in various physicochemical parameters, and the data critically discussed to the protein adsorption in single protein model solutions. Emphasis

is especially given to discuss experimental conditions to obtain results, which are possibly meaningful for the *in vivo* interaction. The results presented here are also of interest for implants made from polymeric biomaterials, i.e., their biocompatibility depending e.g. on the type of proteins adsorbed (opsonins and inflammation versus dysopsonins such as human serum albumin (HSA) and shielding effect).

## 2. Methods

### 2.1 Particle synthesis and purification

As described earlier (Wischke et al., 2013), miniemulsions containing 2 g of monomers or co-monomer mixtures (AN ≥ 99%, NVP ≥ 99%, both purified prior to use), 200 mg hexadecane (≥ 99%), 40 mg 2,2-azobis(2-methyl-butyronitrile) [≥ 98%], and a dispersion medium of 38 ml water supplemented with 80 mg SDS (≥ 99%) were prepared by sonication (90% Amplitude, Sonopuls HD 2017 with a 70 G probe; Bandelin, Berlin, Germany) in an ice bath (all chemicals purchased from Sigma-Aldrich, Steinheim, Germany). Polymerization to PAN nanoparticles was performed at 77 °C under stirring for 7 h. Diluted suspensions were dialyzed (Visking type 20/32 membrane tubing, Carl Roth GmbH, Germany) against 2.5 l of deionized water for 6 days at room temperature. The particle concentration was in the range of 2.7 to 5.3 $mg \cdot ml^{-1}$ after dialysis, with a standardized concentration of 3 $mg \cdot ml^{-1}$ being used in single protein adsorption experiments.

### 2.2 Analysis of copolymer composition and molecular weight

The copolymer composition was determined by $^{1}$H-NMR using lyophilized samples (500 MHz, DMSO-d6). The NVP and AN contents were calculated by x(NVP) = 100-x(AN) and $x(AN) = (I_{2.35\text{-}1.50} - 6 \cdot I_{4.4\text{-}4.0}) \cdot (I_{2.35\text{-}1.50} - 4 \cdot I_{4.4\text{-}4.0})^{-1}$ based on the peak assignment reported before (Wan et al., 2005). The numbers given in the sample codes correspond to the determined NVP content, e.g., PAN 10.8 as copolymer nanoparticles comprising 10.8 mol-% NVP (a precision of the method in the range of ± 3 mol% should be considered).

Gel permeation chromatography (GPC) of filtered samples (0.20 µm PTFE syringe filters) was conducted at 250 x 4.6 mm GRAM gel columns (300 nm and 3 µm porosity, 10 µm gel; Polymer Standard Service GmbH, Mainz, Germany) at 35 °C with a flow rate of 0.25 ml·min$^{-1}$ using dimethylformamide with 50 mmol ammonium acetate as eluent.

2.3 Characterization of particle size and morphology

Particle size and size distribution were determined by dynamic light scattering (DLS) using a Delsa™ Nano C (Beckman Coulter, Krefeld, Germany). Prior to the measurement, 50 µl of the suspension of nanoparticles were diluted with 1 ml of deionized water. The measurements were performed at room temperature using quartz glass cuvettes (Quartz glass SUPRASIL®, 3500 µl, Type 100-QS, Hellma Analytics, Müllheim, Germany).

The morphology of the nanoparticles was evaluated by scanning electron microscopy (SEM) using a Gemini SupraTM 40 VP (Carl Zeiss NTS GmbH, Oberkochen, Germany) at 10 kV with a secondary electron detector. Sample preparation involved a 10fold dilution of the nanoparticle suspension and a spreading of the samples on a glass slide of 10 mm diameter using a spin coater at 5000 rpm for 30 seconds (Laurell Spin Coater Modell 650).

2.4 Analysis of surface charge

The surface charge of nanoparticles was estimated by measuring the zeta potential using a Delsa™ Nano C (Beckman Coulter, Krefeld, Germany). Prior to the measurement, 50 µl of the suspension of nanoparticles were diluted with 1 ml of the different media employed, deionized water and citrate plasma (pooled; DRK – Deutsches Rotes Kreuz, Germany). The measurements were conducted at room temperature using the Standard Flow cell (Beckman Coulter, Krefeld, Germany). Additionally, a pH profile of each sample was recorded from pH 2 to pH 9 with manual adjustment of pH for fresh sample aliquots using sodium hydroxide (Sodium hydroxide solution, 0.1 N, Merck KGaA, Darmstadt, Germany) and hydrogen chloride (Hydrogen chloride, 0.1 N TitriPUR®, Merck KGaA, Darmstadt, Germany).

2.5 Residual surfactant

*2.5.1 X-ray photoelectron spectroscopy (XPS).* Prior to the measurement, nanoparticle suspensions were dried on glass slides to create film-like deposits. The measurement was performed in a XPS spectrometer Axis Ultra of Kratos Analytical Ltd. (Manchester). A monochromatic Al k-alpha radiation was used as energy source (emission 5 mA; anode HT 15 kV). All spectra were recorded at a pass energy of 160 eV with dwell times of 0.1 seconds (survey scans) and 0.25 seconds (region scans). The removal of polymer surface layers was carried out with an ion gun at a pressure of $3 \cdot 10^{-6}$ Torr using two different modes (PAH-mode at 8 kV acceleration HT using coronene, and Ar-mode at 5 kV acceleration HT using Argon).

*2.5.2 High-resolution molecular absorption spectrometry.* For sulfur determination, an experimental setup (developed at Leibniz-Institut für Analytische Wissenschaften, ISAS, Berlin) based on a ContrAA 600 Spectrometer (Analytik Jena AG, Jena, Germany) was used, which comprises a miniaturized graphite tube of 2 mm in diameter and a unique auto-sampler for accurate handling of small sample volumes down to 30 nl. For analysis of the molecular absorption of formed CS as measured at 257.9567 nm, a pyrolysis temperature of 600 °C and a vaporization temperature of 2100 °C were employed. 1% calcium solution was utilized as a matrix modifier. The samples did not need any treatment before the measurement.

2.6 Characterization of particle hydrophobicity

*2.6.1 Contact angle (dry state).* To estimate the hydrophobicity of the nanoparticles, a Droplet Shape Analyzer 100 (Krüss, Germany) equipped with a video camera was employed. Prior to the measurement, 1 ml of the nanoparticles suspension was spread and dried on circular glass slides with a diameter of 22 mm. A drop of water was placed on the dried samples and the contact angle was determined by picture analysis.

*2.6.2 Rose Bengal chromatographic adsorption assay.* Increasing concentrations of nanoparticles (0.5 - 1 - 1.5 - 2 - 2.5 - 3 $mg \cdot ml^{-1}$) with a fixed concentration of 20 $\mu g \cdot ml^{-1}$ of Rose Bengal dye (Rose Bengal sodium salt; dye content ≥ 85%, Sigma Aldrich, Steinheim, Germany) were incubated for 20 min at room temperature. After the incubation period, the samples were centrifuged in a Biofuge Stratos 230V 50/60 Hz (Heraeus, Germany) at 23,300 rpm (50,377 x g) for 15 min. The supernatant was collected using a syringe. The absorbance of unbound dye was measured at 549 nm (Cary 50 Bio UV/Vis spectrometer, Varian) after a 1:4 (v/v) sample dilution with deionized water and compared to a standard curve of the dye.

*2.6.3 Hydrophobic interaction chromatography (HIC).* The HIC was performed using a column C 10/20 (Pharmacia Biotech, Sweden) filled with octyl agarose (Octyl-Sepharose, Sigma-Aldrich). Particle suspensions containing 0.1 mg particles were eluted with MilliQ® water (18.2 MΩcm, MilliQ® system, Millipore, Germany). The elution medium was pumped with a velocity of 2 $ml \cdot min^{-1}$ (Knauer Pump Type 6400). The elution peaks were recorded by UV reading (Kontron Instruments Detector 430) at 300 nm.

*2.6.4 Two phase partitioning (TPP).* TPP was performed by partitioning nanoparticle dispersions in a two phase system. The two phase system was formed by mixing equal amounts of 12% (m/v) polyethylene glycol (PEG) 2000 (Fluka) and 16% (m/v) dextran FP 40 (SERVA Electrophoresis) in a tube (12 ml). The nanoparticle concentrations were determined in each phase applying UV reading, whereby partitioning equilibrium was reached after 24 h. To exclude particle aggregation during partitioning, z-averages (Zetasizer Nano ZS) were measured after 24 h. From this, the samples PAN 6.8 (size: +50%) and PAN 33.8 (+32.3%) had to be excluded from this analysis due to strong particle aggregation in the PEG phase (limit was +12.5%). All measurements were repeated three times.

## 2.7 Single protein adsorption

*2.7.1 Sample incubation.* Bovine serum albumin (BSA) and fibronectin (FN) were purchased from Sigma Aldrich (Steinheim, Germany) and used at different concentrations for BSA (40 $mg \cdot ml^{-1}$) and FN (400 $\mu g \cdot ml^{-1}$). A concentration of 3 $mg \cdot ml^{-1}$ of nanoparticles was incubated with each protein solution at 37 °C for 24 h. After the incubation period, the mixtures were centrifuged in a Biofuge Stratos 230V 50/60 Hz (Heraeus, Germany) at 23,300 rpm (50,377 x g) for 45 min. The supernatant and pellet were separated using a 1 ml syringe and the pellet was freeze-dried.

*2.7.2 Bicinchoninic acid (BCA) assay.* For analysis of the protein concentration of the supernatant, the QuantiPro™BCA Assay kit (Sigma Aldrich, Steinheim, Germany) was used. 100 µl of the supernatant were mixed with 100 µl of the BCA reagent in a 96 well plate and incubated for 3 hours at 37 °C. A standard curve from 0–75 $\mu g \cdot ml^{-1}$ of each single protein was handled along with the samples. If necessary, the samples were diluted for measurement. The absorbance was measured at 562 nm using a microplate reader (Infinite® 200 PRO, Tecan, Switzerland).

*2.7.3 HPLC amino acid analysis*. The quantity of adsorbed protein on the pellet was determined after acidic hydrolysis of the proteins, for which freeze dried samples were incubated with 1 ml of 6N HCl at 115 °C for 24 h using a digital dry block heater. The sample volume was subsequently adjusted to 10.0 ml using deionized water, of which 500 µl were adjusted to neutral pH by adding 300 µl of 1N NaOH. After centrifugation (10,800 x g, 5 min), samples were analyzed on an Agilent Technologies 1200 HPLC with pre-column derivatisation with ortho-phosphoric acid (OPA) and fluorenylmethyloxycarbonyl chloride (FMOC) reagent and separation on an ZORBAX Eclipse Plus C18 column (3.0 x 250 mm, 5 µm; with corresponding guard column; Agilent) according to the Agilent application note. Separation was performed at a flow of 0.64 $ml \cdot min^{-1}$ at 40 °C with a gradient of 2% to 100%

of solvent A (ACN:MeOH:Water = 45:45:10) against solvent B (10 mM $Na_2HPO_4$, 10 mM $Na_2B_4O_7$, 5 mM $NaN_3$; pH 8.2).

## 3. Results and Discussion

### 3.1 Nanocarrier synthesis and analysis of bulk polymer composition and particle size

The curvature of a particle surface can affect the adsorption of compounds such as proteins. It is known that proteins have different affinities to flat and curved surfaces (Lynch and Dawson, 2008), which can also affect their conformation in the adsorbed state (Lundqvist et al., 2004) and exposure of distinct moieties to the surrounding medium, e.g. charged or hydrophobic groups. To minimize this potential influence, miniemulsion polymerization was selected to prepare nanoparticles in a size range as close as possible, i.e. ranging from about 130 to 180 nm (z-averages in dynamic light scattering; Table 1). As seen by the polydispersity indices (PI), they possessed a relatively narrow size distribution. These data were well in agreement with the SEM analysis, which showed spherical particles of homogeneous sizes (Fig. 1). The bulk composition of the polymer nanoparticles was determined by $^1$H-NMR and showed a systematic alteration as intended. The semi-crystalline morphology of polyacrylonitrile resulted in surface roughness of nanoparticles with low NVP content, which is eliminated at higher NVP content. The small effect of surface roughness on the available surface area for protein adsorption was neglected in this study.

**Table 1:** Overview on nanoparticle bulk composition and size characterization data from DLS (z-average, polydispersity index [PI]) and determination of sulfur in nanoparticle suspensions.

| Sample | Composition | Particle size | | Sulfur concentration |
|---|---|---|---|---|
| | NVP content [mol-%] [1] | z-average [nm] [2] | PI [2] | [µg·ml$^{-1}$] [3] |
| PAN 0 | 0 | 181 | 0.07 | 0.6 ± 0.1 |
| PAN 6.7 | 6.7 | 165 | 0.08 | 0.8 ± 0.1 |

| | | | | |
|---|---|---|---|---|
| PAN 6.8 | 6.8 | 170 | 0.05 | 1.0 ± 0.1 |
| PAN 10.8 | 10.8 | 170 | 0.12 | 1.6 ± 0.1 |
| PAN 15.1 | 15.1 | 135 | 0.10 | 1.0 ± 0.1 |
| PAN 23.9 | 23.9 | 137 | 0.06 | 0.4 ± 0.1 |
| PAN 27.7 | 27.7 | 146 | 0.08 | 0.3 ± 0.1 |
| PAN 33.8 | 33.8 | 133 | 0.07 | 0.6 ± 0.1 |

[1] Determined by NMR with typical precission of ± 3 mol-%. [2] Data for a minimum of 100 accumulated measurements per sample. [3] Analysis by molecular absorption spectroscopy (n =5, mean, S.D.).

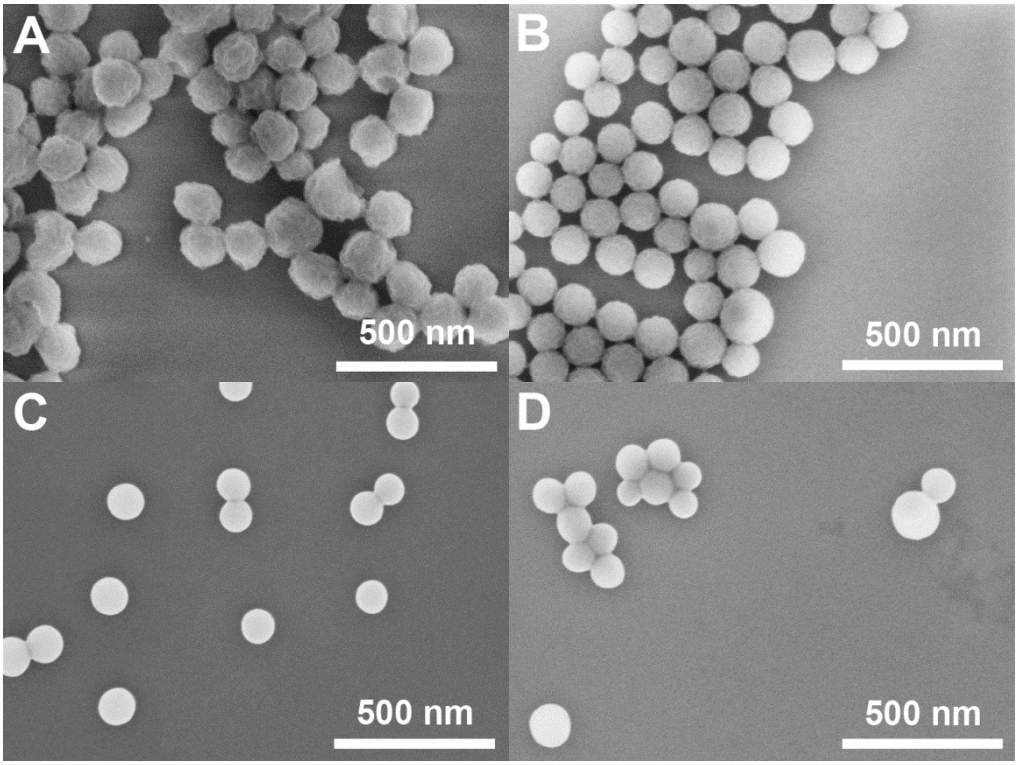


**Fig. 1:** Exemplary SEM images of nanoparticles. (A) PAN 0; (B) PAN 6.7; (C) PAN 23.9; (D) PAN 33.8.

## 3.2 Surface composition and hydrophobicity of nanocarriers

### *3.2.1 Residual surfactant*

SDS, required for the stabilization of droplets in the miniemulsion, may remain associated to the particle surface after completion of the nanoparticle synthesis. While being expected to be mostly removed from the particle suspension during dialysis, potential larger quantities of

residual SDS might result in a dominant effect of SDS rather than the copolymer composition at the particle interface layer. This includes potential contributions of anionic charge being introduced by the dissociated organosulfate salt.

In a previous study, elemental analysis suggested a sulfur content of 1 wt-% (Li et al., 2012), which appeared very high compared to the initially used SDS in the synthesis and therefore needed to be reconsidered. Here, different approaches were followed to assess SDS quantities in the nanoparticle suspension: i) the determination of sulfur as characteristic element of SDS by XPS on dried nanoparticle suspension on a glass substrate, and ii) high-resolution AAS using the molecular adsorption lines of carbon monosulfide formed from sulfur in a fuel-rich air-acetylene flame upon injection of nanoparticle suspensions (Heitmann et al., 2006). Nanoparticle suspensions were dried on glass substrates and analyzed by XPS at several angles to collect information from different sample depth in the range of 2-8 nm. Despite analysis was conducted at different sample positions, angles, and with additionally ion sputtering sources for etching with coronene and argon ions, respectively, no sulfur signal could be detected (Fig. 2). This suggests that the residual content of SDS should be below the detection limit of XPS, which has a sensitivity for sulfur in the range of 800 ppm.

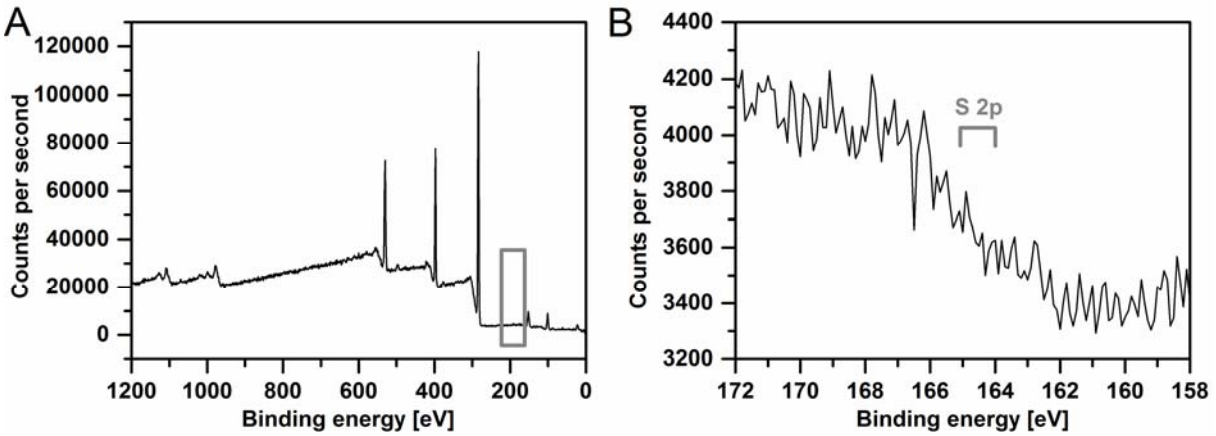


**Fig. 2:** Exemplary spectra of XPS analysis of PAN 0 nanoparticle suspensions dried on glass substrate and subjected to coronene ion bombardment. (A) Overview, (B) Detail of sulfur 2p region.

As another method of determining sulfur, a modified atom adsorption spectroscopy method was applied. This technology was recently extended to a sensitive quantitative determination of the molecular adsorption of sulfur derivatives like CS formed *in situ* in miniaturized graphene tubes under distinct pyrolysis conditions. As shown in Tab. 1, the concentration of sulfur in the nanoparticle suspension was generally very low. Based on a sulfur content of <2 ppm, an SDS content <18 ppm can be concluded. There were no large differences of sulfur content detected for the different sample compositions. By trend, the sulfur content was slightly higher for nanoparticles with low NVP content, which previously showed faster endocytosis (Wischke et al., 2013). However, a logical correlation between these two observations remains speculative at this time.

*3.2.2 Challenges in assessing surface hydrophobicity by contact angle analysis and dye adsorption*

Based on the different physicochemical properties of homopolymers of AN and NVP, it can be expected that a series of copolymers with increasing NVP content would result in increasing hydrophilicity. As described above, the interface composition may not necessarily reflect the bulk composition and an experimental characterization of hydrophobicity is needed. An often followed approach is the measurement of contact angles of films prepared by drying nanoparticle suspensions, which are artifact-prone due to the intermediate drying step as well as their porous structure. For the dried PAN nanoparticles, very low apparent contact angles of ($\theta_{adv}$: 34.7° – 24.0°) compared to the flat glass substrate ($\theta_{adv}$: 72.4°) could be measured. To illustrate their erroneousness, disks from PAN powders were prepared by compression either under low pressure to a sintered porous structure or, at higher pressure, to non-porous surfaces. Substantially lower contact angles were observed for the porous compared to non-porous disks (data not shown). Therefore, it should be noted that capillary forces at interparticulate cavities of dried nanoparticle films may disturbe the analysis of hydrophobicity by contact angle measurements, thus leading to the need of alternative methods.

To evaluate the surface hydrophobicity of the nanocarriers in aqueous dispersion, i.e. in the hydrated state of the surface without intermediate drying, adsorption of reporter molecules such as hydrophobic dyes can be performed. One option is the determination of adsorption isotherms and calculating the binding constant *k* via a Scatchard plot, often performed using Rose Bengal (RB) (Doktorovova et al., 2012; Müller, 1997; Müller, 1991). This procedure is very time consuming. As alternative, the partition quotient *PQ* of RB between the particle surface (phase 1) and the aqueous dispersion medium (phase 2) can be analyzed for increasing particle concentrations, i.e. increasing surface area, at constant RB concentration. If the hydrophobicity is high, *PQ* will strongly increase with increasing surface area, resulting in a steep slope of the obtained curve in a plot of *PQ* versus surface area. If the particles are hydrophilic, the slope is low and in some cases the line is almost parallel to the x-axis (Müller, 1997). In Fig. 3, the slope of the fitted curves from the *PQ* plot are presentend also including reference data for polystyrene nanoparticles (PS; 60 nm) and PS nanoparticle surfaces modified with carboxy groups (PS-COOH) as taken from (Müller, 1991). Compared to the hydrophobic PS sample, all PAN nanoparticles are very hydrophilic with values close to that of PS-COOH. Interestingly, preliminary screening experiments showed, in contrast to our expectation, a trend towards higher binding of RB for theoretically more hydrophilic samples of a higher NVP bulk content, Possible explanations may be a contribution of specific interaction of anionic RB with the amphiphilic NVP (Klotz and Shikama, 1968) (Maruthamuthu and Sobhana, 1979) compared to a theoretically repulsion from AN in case of a possible partial hydrolysis of nitrile groups to carboxyl functions at the nanoparticle surface (Ermakov et al., 2000). This may have led to a condition where the RB adsorption pattern was indicative of the NVP content at the surface rather than the nanoparticle hydrophobicity, which is why this assay was not further employed here.

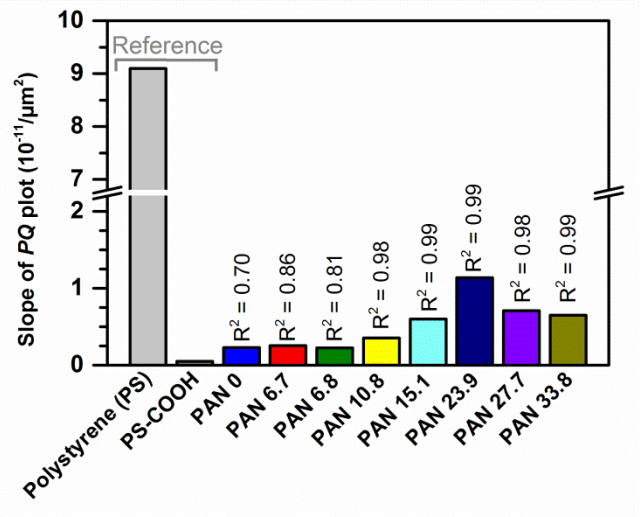


**Fig. 3:** Rose Bengal adsorption assay to characterize particle hydrophobicity. Plotted is slope of *PQ* plot [$x10^{-11} \cdot \mu m^{-2}$] as derived from a series of individual partition experiments for each of the different nanoparticle compositions ($R^2$ is the correlation coefficient from linear regression to determine the respective slope). The indicated reference data are reprinted from (Müller et al., 1986) with kind permission from Springer Science and Business Media.

*3.2.3 Analysing nanoparticle surface hydrophobicity by chromatography*

Hydrophobic interaction chromatography (HIC) is another methodology that can be applied to characterize nanocarriers in their hydrated state. Based on the elution profiles (Fig. 4) for the different particle types, particularly when looking only at the retention times of the peak maxima (Fig. 5), one cannot clearly differentiate the nanoparticles in terms of hydrophobicity. It can be concluded that the particles:

i) are relatively hydrophilic in absolute terms because they can be eluted at reasonable elution times from the hydrophobic octyl-Sepharose columns, and

ii) are very similar because the peaks eluate on the same column at the same retention time.

For PAN 0, PAN 6.7 and PAN 33.8, an almost monomodal hydrophobicity can be concluded, as indicated by their narrow main peaks with only minor side peaks. This can be also seen by the relatively close peak set off times (Fig. 5). In contrast, the sample PAN 23.9 shows a very high peak set off time, which reflects a higher broadness of this peak. This indicates

different fractions of particles in this sample, which are either more hydrophilic (main peak) or more hydrophobic (tail of the peak), possibly due to a lower SDS presence on the particle surface. PAN 6.8 shows a profile where clearly 3 different fractions of hydrophobicity can be seen (trimodal): a more hydrophilic fraction (left shoulder of main peak) and a more hydrophobic fraction (3rd peak at approx. 30 min). Considering that this sample has the highest residual SDS content of the here investigated materials, it may be possible that the SDS is very heterogenically distributed on the particle surfaces. In general, one can see that peak onset times are close to the peak maxima, whereby peak offset times have a larger difference to maxima (peak tailing).

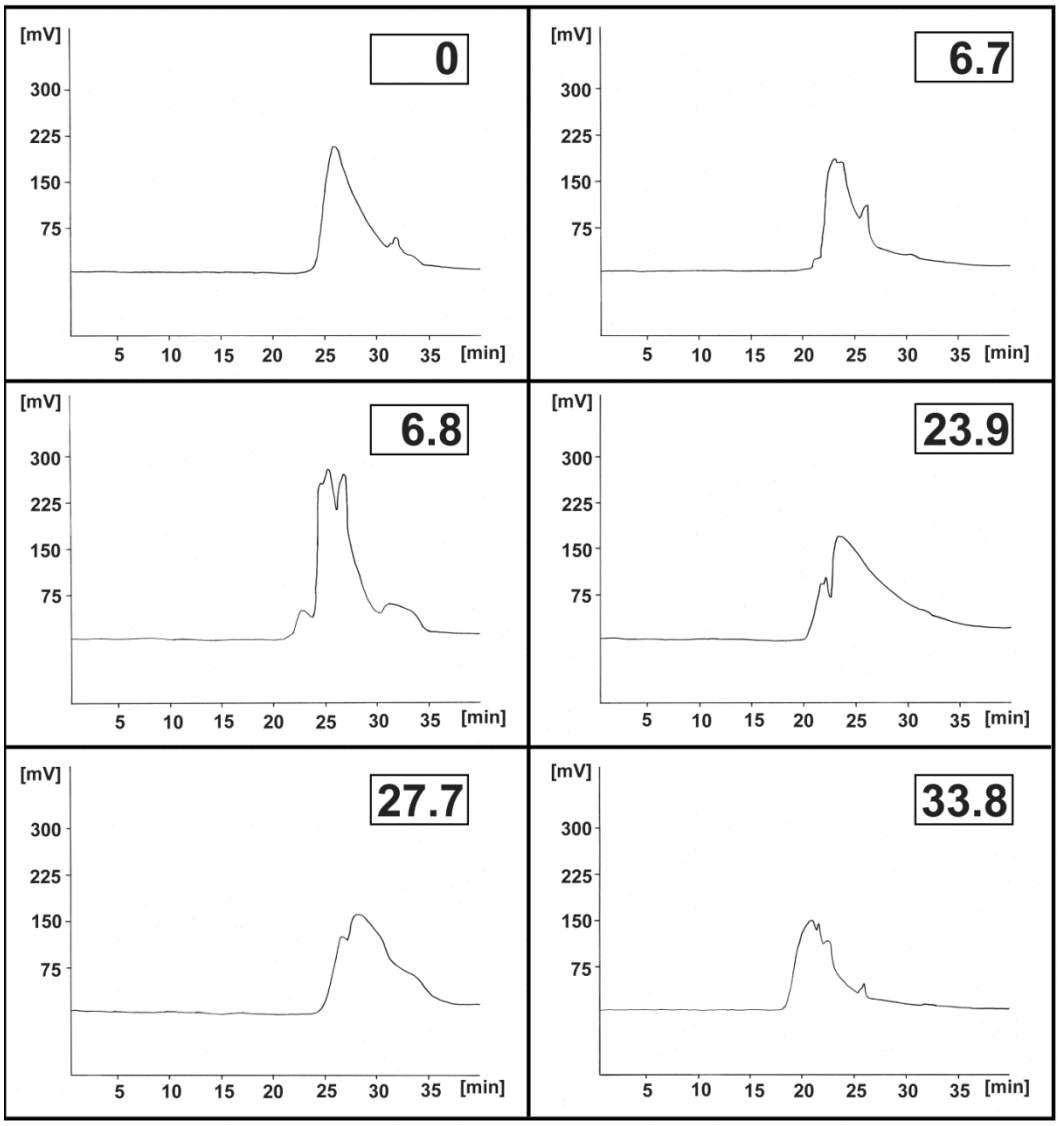


**Fig. 4:** Elution profiles from octyl-Sepharose HIC. The legend shows NVP molar contents for different PAN samples.

Based on these results, it can be summarized that the change in co-monomer content did not led to pronounced differences in hydrophobicity as theoretically expected. The different co-polymer content could not be reflected in the HIC results because of a similar presence of hydrophilic groups at the particle surface. In addition to any hydrophilic groups originating from the matrix polymer, the residual SDS content, despite being low, may be relevant here due to the strong polar ionic sulfate groups at the outer shell of the particles. Interestingly, PAN 27.7 having the lowest SDS residue showed the highest retention (peak maxima), possibly because a lower number of polar sulfate groups were exposed at the surface of these particles.

However, the observed distinct differences detectable by HIC (broadness and shape of peaks, modality) are not straightforward explainable due to superimposing effects of polymer composition and remaining SDS on the surface. Still, the HIC results suggest that hydrophobic interactions rather than size exclusion effects of nanoparticles possible in agarose-based gels (Göppert and Müller, 2004) played the dominant role in the performed analysis. The PAN 33.8 nanoparticles with the smallest z-ave of 133 nm were eluted the fastest (regarding to peak maxima), whereby it would be the opposite in case of size exclusion. Anyhow, the detected differences particularly in peak shape and width show the power of the HIC method to assess even small differences in hydrophobicity.

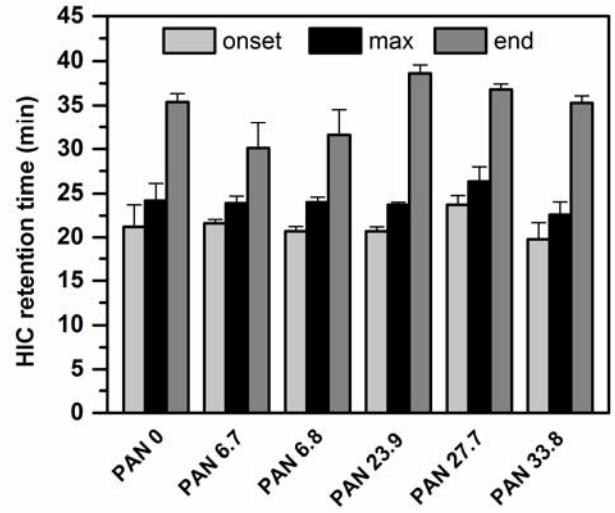


**Fig. 5:** HIC retention times of particles with different NVP content from Octyl-Sepharose HIC (n=3). Given is the onset, maximum and end of the respective peak.

*3.2.4 Two phase partitioning (TPP)*

TPP is described to be a suitable hydrophobicity determination method for very hydrophilic particles (Müller, 1991). Relative to each other, the used PEG-rich phase is more hydrophobic than the dextran-rich phase. Accordingly, decreasing concentrations of particles in the PEG-rich phase will indicate a reduced surface hydrophobicity. TPP analysis (Fig. 6) revealed a decreasing amount of particles found in the PEG phase with increasing NVP content from 0 to 27.7 mol-% (note: the other compositions aggregated and data could not be properly evaluated). This is reflecting that particles becoming less hydrophobic with increasing amount of the hydrophilic repetitive unit NVP. While HIC showed similar retention times and thereby could not differentiate between different hydrophilicities, the partitioning in the polymer solutions could reflect the different co-monomer content. A possible explanation is that SDS, which might have affected the interaction in HIC analysis, seems to play a minor role during partitioning in the TPP assay.

In principle, the hydrophobicity can be quantified by different types of interactions, i.e. the affinity of a hydrophobic dye to a surface (RB assay), the interaction with a hydrophobic carbon chain (HIC), and interactions with a polyether material (TPP). In analogy to different nanoparticle diameters being often detected when analyzing samples with different methods, different types of interactions appear to dominate experimental results when analyzing surface properties by the different hydrophobicity assays.

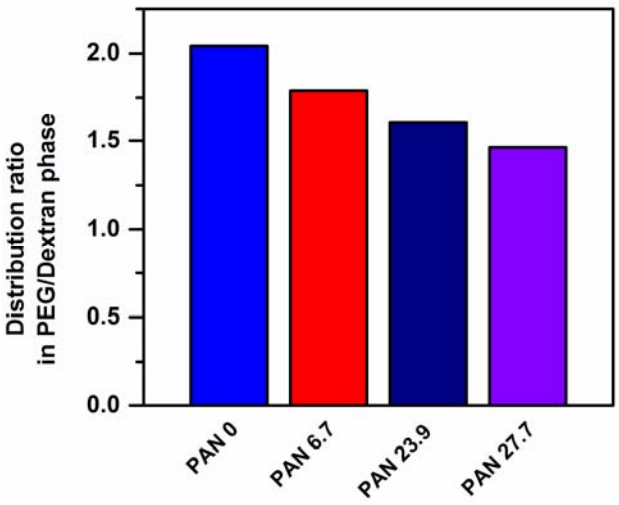

**Fig. 6:** Nanoparticle distribution in two-phase partition (TPP) experiments. Plotted is the ratio of the particle amount found in the PEG-rich phase versus the Dextran-rich phase.

445

## 3.3 Analysis of zeta potential in different microenvironments

### *3.3.1 Zeta potential in water of different pH*

Besides hydrophobicity, surface charge is a relevant property for the fate of nanocarriers in a biological system. The zeta potential (ZP) of nanocarriers is a standard property measured to
450 estimate the surface charge of the particles (NERNST potential), which cannot be easily determined. Importantly, the measuring conditions by laser Doppler anemometry are absolutely crucial to allow conclusions to the charge situation at the surface. In particular, a potential at the particle surface as close as possible to the STERN layer needs to be measured, which has a correlation to the surface potential (the higher the Stern potential, the
455 higher is the charge on the surface).

Since the ZP differs from the Stern potential according to an exponential decay curve defined by the ion type and concentration in the diffuse layer, the original nanoparticle charges should be determined without using salts or buffers in the suspension medium. Thus, the ZP was first measured in distilled water having a conductivity of 50 $\mu S \cdot cm^{-1}$. While distilled water
460 has conductivities fluctuating typically between 1 and 10 $\mu S \cdot cm^{-1}$ that can lead to fluctuating ZP values, a very low basis conductivity of 50 $\mu S \cdot cm^{-1}$ realized by NaCl addition allows to avoid such experimental difficulties (for details cf. (Lucks et al., 1990)). Under these conditions, the obtained ZP is practically identical to the Stern potential. Here, the absolute values should be considered, that means e.g. an alteration from -30 mV to -40 mV is to be
465 considered as an “increase” of charge.

The analysis yielded a ZP of about -27 mV for the NVP-free nanoparticles PAN 0 with a stepwise increase to values of about -30 to -40 mV for the nanoparticles containing NVP (Table 2). This pattern was found to show no direct correlation with the residual SDS content of the PAN nanoparticles. This suggests that the zeta potential is not primarily a function of

NVP content or of the residual SDS, but may be affected by combination of those two parameters. Additionally, unidentified reactions might potentially contribute to the charge at the particle surface such as partial hydrolysis of nitrile moieties to acrylamides or acrylic acids (Krentsel et al., 2001) or, as described for harsh conditions, partial hydrolysis of the lactam rings of NVP to the corresponding amino acid derivative (Conix and Smets, 1955).

**Table 2:** Zeta potential (ZP) of nanoparticles depending on the properties of the aqueous suspension medium. Data of ZP (n≥3 repetitive measurements, mean ± SD), conductivities (conduct.) of the suspension medium, and the calculated points of zero charge are shown (PZC).

| | **Analysis in water[1]** | | **Analysis at ~pH 7.4[2]** | | **Analysis at pH ~2.1[2]** | | |
|---|---|---|---|---|---|---|---|
| **Sample** | **ZP [mV]** | **Conduct. [µS·cm$^{-1}$]** | **ZP [mV]** | **Conduct. [µS·cm$^{-1}$]** | **ZP [mV]** | **Conduct. [µS·cm$^{-1}$]** | **PZC[3]** |
| **PAN 0** | -29.5 ± 1.5 | 52 | -29.6 ± 0.4 | 32 | +20.8 ± 0.4 | 630 | 4.1 |
| **PAN 6.7** | -30.8 ± 1.3 | 55 | -25.0 ± 0.5 | 534 | +21.4 ± 0.5 | 2330 | 3.4 |
| **PAN 6.8** | -35.3 ± 1.7 | 51 | -31.7 ± 1.6 | 73 | +16.9 ± 1.1 | 1090 | 2.9 |
| **PAN 10.8** | -39.5 ± 6.3 | 51 | -40 ± 0.4. | 35 | -2.3 ± 0.4 | 540 | n.d. |
| **PAN 15.1** | -34.6 ± 0.8 | 51 | -29.7 ± 0.9 | 44 | +0.7 ± 0.2 | 795 | 2.6. |
| **PAN 23.9** | -43.1 ± 2.0 | 51 | -29.5 ± 0.3 | 1617 | +5.0 ± 1.0 | 7970 | 3.6 |
| **PAN 27.7** | -41.0 ± 1.5 | 54 | n.d. | n.d. | +4.4 ± 1.0 | 3390 | 2.9 |
| **PAN 33.8** | -44.2 ± 3.1 | 49 | n.d. | n.d. | +2.7 ± 0.2 | 1280 | 3.4 |

[1] In this series of measurement, only the conductivity was adjusted by NaCl addition. The pH was around pH 6. [2] The pH was adjusted by adding HCl or NaOH solution to a value of roughly pH 2.1 ± 1 or pH 7.4± 1 with the given deviations due to the exclusion of buffering salts. The conductivity was monitored as indicated. [3] Calculated or estimated from profile shown in Fig. 7. n.d. = not determined;

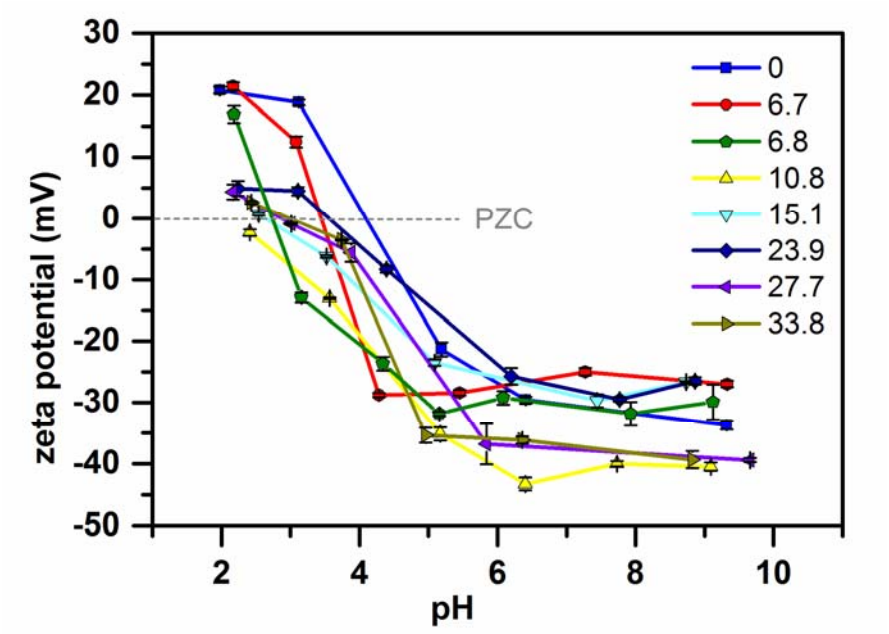


**Fig. 7:** ZP-pH profiles of the model nanocarriers as determined by manual adjustment of the pH with NaOH/HCl without the use of buffers. Legend shows NVP molar contents for different PAN samples.

The pH can strongly affect the surface charge by pH dependent dissociation of functional groups and adsorption of $H^+$ and $OH^-$ ions. Thus, ZP analysis was also performed after pH adjustment by HCl and NaOH addition (which automatically results in modified conductivity; no buffers to be used). After pH adjustment to ~pH 7.4, less negative ZP values were detected in most cases illustrating the effect of ions added into the suspension medium (Table 2). Again, by trend and with few exceptions, nanoparticles with higher NVP content showed higher values of negative charges than samples with low NVP content. From this, different electrostatic interactions with distinct proteins in solution at pH 7.4 can be expected (Engberg et al., 2015).

The points of zero charge (PZC) (compare Table 2) as estimated from the ZP-pH profiles (Fig. 7) differ clearly for nanoparticles only composed of acrylonitrile (PZC at pH 4.1) and the formulations containing NVP (PZC at around pH 3.0-3.5), but no straight forward correlation

between PZC and NVP content exists. However, distinct differences were found in the protonability at pH below the PZC. The ZP reverses to positive values for all nanoparticle compositions, while adapting values of around +20 mV for samples with low NVP content but only +5 mV for NVP contents >10 mol-% (Table 2). The alteration of particle charge depending on the environmental pH may suggest that some particles may act similar regarding electrostatic interaction with proteins, some different, at relevant pH differences in the body e.g. pH 7.4 in the blood, about pH 5 in phagolysosomes or even lower pH in inflamed regions.

When comparing PAN 6.7 and 6.8 as samples of practically identical composition, a fair level of reproducibility of the particle production could be concluded. This demonstrates the strength of ZP analysis in routine control of particle reproducibility, which may be further expanded to 3-D scans measuring the ZP (y axis) as function of pH (x-axis) and at the same time of increasing electrolyte concentration (z axis), e.g. NaCl (Paulke et al., 1995).

*3.3.2 Nanocarrier charge (ZP) in citrate plasma*

Early studies in the 1950ies explored the effect of the charge of injected particles on their body distribution. For example, it was found that positively charged particles were cleared fastest by the reticuloendothelial system (RES), while negatively charged particles were cleared more slowly and particles with little charge relatively slowest (Wilkins and Myers, 1966). However, it was neglected in these studies that after injection into the blood, nanoparticles adsorb blood proteins, which changes their original charge (ZP). The blood proteins adsorb on the particle surface, either on the firmly fixed Stern layer (forming a third layer on the inner and outer Stern layer) or by replacing the ions in the inner and outer Stern layer, i.e. changing the composition of the Stern layer. The associated change in surface charge is an indicator i) how much protein adsorbed and/or ii) if less or more charged proteins adsorb (blood protein charge is a function of their isoelectric point (IEP) related to the blood pH).

Therefore, the ZP was additionally determined in plasma. Measurements were also performed as a function of time (Table 3), because it is known that the adsorbed protein composition in the blood changes with time (Göppert and Müller, 2005). The most hydrophobic nanocarriers PAN 0 exhibited a low ZP in plasma of about -5 mV, which is similar to the low ZP of previously reported stealth nanoparticles with extended circulation time (Gref et al., 2000). The particles with increasing NVP content showed higher zeta potential values in the range -8 mV to -13 mV (Table 3, at 0 hours).

Early studies with polystyrene nanoparticles, either uncoated (ZP around -15 mV; fast liver clearance) or Poloxamine 908-coated (ZP around -5 mV; extended blood circulation and high adsorption of albumin as dysopsonin) suggested that a higher charge in plasma (Müller, 1991), i.e. more adsorption of charged proteins, would mean a faster recognition by the RES. Based on the scale from -5 mV to -15 mV, there is no clear relationship in this study between ZP and increasing content of NVP or the measured hydrophobicity. PAN 0 (most hydrophobic in TPP assay) and the PAN 27.7 (most hydrophilic in TPP assay) had both a low ZP of about 5-8 mV. From this it is concluded, that in this case, the ZP values in plasma have limited power towards a systematic categorization of the investigated nanoparticles. It has to be stressed that not only the quantitiy, but in particular the type of adsorbed protein can be of relevance for biological recognition of nanocarriers. With increasing incubation time, the measured ZP changed adapting values of about -8 mV after 6 hours for most formulations (Table 3). This can be explained by the protein adsorption kinetics. First more abundant blood proteins adsorb despite having low affinity, which are later being gradually replaced by proteins with higher affinity that may be present in serum only at low concentrations (Blunk et al., 1996; Harnisch and Müller, 2000; Wei et al., 2014).

**Table 3:** ZP of the nanocarriers measured in citrate plasma immediately after mixing (0 hours) and at later time points.[1]

| | ZP in citrate plasma (mV) | | |
|---|---|---|---|
| **Sample** | **0 h** | **1 h** | **6 h** |
| PAN 0 | -4 | -5 | -6 |
| PAN 6.7 | -8 | -6 | -8 |
| PAN 6.8 | -10 | -9 | -7 |
| PAN 23.9 | -13 | -8 | -8 |
| PAN 27.7 | -8 | -10 | -8 |
| PAN 33.8 | -7 | -5 | -3 |

[1] Data are derived from a single analysis with pooled citrate plasma. The analysis involves the measurement in five positions of the electrophoretic channel. The typical methodological error of zeta potential measurements is <± 2 mV.

## 3.4 Single protein binding to the nanocarriers

Considering the relevance of nanoparticle interaction with specific proteins, adsorption studies in solutions of single proteins can indicate the basic affinity of a single protein to different surfaces. Binding studies in albumin solution (in this case bovine serum albumin, BSA) were therefore conducted to assess if albumin has indeed a high affinity to the PAN 0 nanocarriers as assumed from the low ZP in plasma of only -5 mV. Fig. 8 shows that PAN 0 had the highest adsorption of albumin. E.g., PAN 23.9 exhibited the lowest adsorption of albumin being in agreement with the relatively high ZP of around -13 mV, which could potentially give more charged apolipoproteins a chance to adsorb with time. In addition, the adsorption of fibronectin as an adhesive glycoprotein involved in cellular recognition of biomaterials was studied. Again, the most excessive protein adsorption exhibited PAN 0, the most hydrophobic nanocarriers (as measured by the TPP assay).

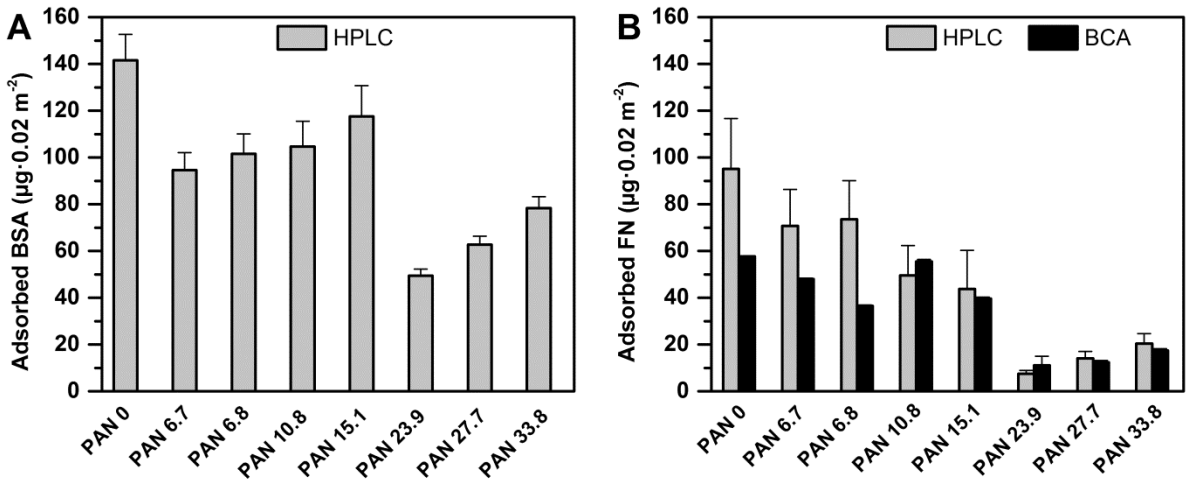


**Fig. 8:** Single protein adsorption studies using protein solutions corresponding to the concentrations present in human blood plasma for (A) bovine serum albumin (BSA; 40 mg·ml$^{-1}$) and (B) fibronectin (FN; 400 µg·ml$^{-1}$). The adsorbed protein on the nanoparticle surface was determined by amino acid analysis by HPLC (n=6 amino acids quantified, S.D.). Additionally BCA assay of the non-adsorbed protein fraction was performed for FN (n=3 quantifications, S.D.).

## 4. Conclusions

In this study, a series of PAN model nanoparticles was synthesized to expand the set of model nanoparticles available for mechanistic studies of protein adsorption beyond polystyrene based latices. From chemistry considerations related to bulk composition, it could be speculated that the surface hydrophobicity should decrease with increasing content of the comonomer *N*-vinyl pyrrolidone (NVP). Reexamining this prediction indicated that there exists no straightforward relationship of a reducing hydrophobicity with increasing NVP content. The relationship seems to be rather complex and may include i) the presence of adsorbed substances like surfactants, ii) chemical alteration of moieties at the surface, and/or iii) a non-linear correlation of bulk composition and surface exposure of the two repetitive units.

The analysis of surface hydrophobicity by contact angles of films derived by nanoparticle drying is believed to be strongly artefact prone, which is why a comprehensive wet-state

analysis was applied. A very low hydrophobicity of all PAN nanoparticles compared to polystyrene nanoparticles was indicated by the Rose Bengal assay. Aqueous two-phase partitioning experiments were best suited to distinguish the decrease in hydrophobicity for the investigated increasing NVP content. HIC revealed that some particle formulations are of monomodal hydrophobicity, either having a narrow or a broad distribution. In some cases, however, trimodal HIC distributions were detected – i.e. an indication of "polydispersity of surface hydrophobicity". Despite the content of residual SDS surfactant in the nanoparticle suspensions was in the very low 1 ppm range as determined by molecular absorption spectroscopy of a sulfur derivative, clustering of SDS on the surface of distinct nanoparticle populations cannot be excluded. Such subpopulations can be of high relevance as they might show a different interaction with biomolecules like proteins and eventually an altered organ distribution in vivo. The characterization of particle charge by analyzing zeta potentials (ZP) illustrated a ZP reduction e.g. for PAN 0 from about -30 mV in water to -5 mV in plasma by the formation of a hydrophilic protein corona. Single protein adsorption analysis allowed to confirm that the PAN 0 nanoparticles were adsorbing the largest quantity e.g. of albumin. Considering protein exchange processes as indicated by zeta potential analysis over time and the potential dominance of biological function mediated by specific proteins adsorbed at low quantities, the next steps will be the assessment of the complete adsorption pattern in plasma and eventually in vivo organ distribution to have the full correlation of in vitro characterization data, protein adsorption pattern, and organ distribution.

**Acknowledgements**

The authors thank for the support by Dr. T. Weigel (XPS analysis) and the discussion with Dr. Florek in preparation for sample characterization by molecular absorption spectroscopy. Discussion with F. Störmann and Dr. A Neffe during manuscript preparation is acknowledged.

**References**


Armstrong, T.I., Davies, M.C., Illum, L., 1997. Human serum albumin as a probe for protein adsorption to nanoparticles: relevance to biodistribution. Journal of Drug Targeting 4, 389-398.

Blunk, T., Lück, M., Calvor, A., Hochstrasser, D.F., Sanchez, J.-C., Müller, B.W., Müller, R.H., 1996. Kinetics of plasma protein adsorption on model particles for controlled drug delivery and drug targeting. European Journal of Pharmaceutics and Biopharmaceutics 42, 262-268.

Conix, A., Smets, G., 1955. Ring opening in lactam polymers. Journal of Polymer Science 15, 221-229.

Doktorovova, S., Shegokar, R., Martins-Lopes, P., Silva, A.M., Lopes, C.M., Müller, R.H., Souto, E.B., 2012. Modified Rose Bengal assay for surface hydrophobicity evaluation of cationic solid lipid nanoparticles (cSLN). European Journal of Pharmaceutical Sciences 45, 606-612.

Engberg, A.E., Nilsson, P.H., Huang, S., Fromell, K., Hamad, O.A., Mollnes, T.E., Rosengren-Holmberg, J.P., Sandholm, K., Teramura, Y., Nicholls, I.A., Nilsson, B., Ekdahl, K.N., 2015. Prediction of inflammatory responses induced by biomaterials in contact with human blood using protein fingerprint from plasma. Biomaterials 36, 55-65.

Ermakov, I.V., Rebrov, A.I., Litmanovich, A.D., Platé, N.A., 2000. Alkaline hydrolysis of polyacrylonitrile, 1. Structure of the reaction products. Macromolecular Chemistry and Physics 201, 1415-1418.

Gessner, A., Lieske, A., Paulke, B., Müller, R.H., 2002. Influence of surface charge density on protein adsorption on polymeric nanoparticles: analysis by two-dimensional electrophoresis. European Journal of Pharmaceutics and Biopharmaceutics 54, 165-170.

Gessner, A., Lieske, A., Paulke, B.R., Müller, R.H., 2003. Functional groups on polystyrene model nanoparticles: influence on protein adsorption. Journal of Biomedical Materials Research Part A 65, 319-326.

Göppert, T.M., Müller, R.H., 2004. Alternative sample preparation prior to two-dimensional electrophoresis protein analysis on solid lipid nanoparticles. Electrophoresis 25, 134-140.

Göppert, T.M., Müller, R.H., 2005. Adsorption kinetics of plasma proteins on solid lipid nanoparticles for drug targeting. International Journal of Pharmaceutics 302, 172-186.

Gref, R., Lück, M., Quellec, P., Marchand, M., Dellacherie, E., Harnisch, S., Blunk, T., Müller, R.H., 2000. 'Stealth' corona-core nanoparticles surface modified by polyethylene glycol (PEG): influences of the corona (PEG chain length and surface density) and of the core composition on phagocytic uptake and plasma protein adsorption. Colloids and Surfaces B: Biointerfaces 18, 301-313.

Harnisch, S., Müller, R.H., 2000. Adsorption kinetics of plasma proteins on oil-in-water emulsions for parenteral nutrition. European Journal of Pharmaceutics and Biopharmaceutics 49, 41-46.

Heitmann, U., Becker-Ross, H., Florek, S., Huang, M.D., Okruss, M., 2006. Determination of non-metals via molecular absorption using high-resolution continuum source absorption spectrometry and graphite furnace atomization. Journal of Analytical Atomic Spectrometry 21, 1314-1320.

Klotz, I.M., Shikama, K., 1968. Nature of urea effects on anion binding by macromolecules. Archives of biochemistry and biophysics 123, 551-557.

Krentsel, L.B., Kudryavtsev, Y.V., Rebrov, A.I., Litmanovich, A.D., Platé, N.A., 2001. Acidic Hydrolysis of Polyacrylonitrile: Effect of Neighboring Groups. Macromolecules 34, 5607-5610.

Kreuter, J., Petrov, V.E., Kharkevich, D.A., Alyautdin, R.N., 1997. Influence of the type of surfactant on the analgesic effects induced by the peptide dalargin after its delivery across the blood-brain barrier using surfactant-coated nanoparticles. Journal of Controlled Release 49, 81-87.

Li, W., Pierce, B.F., Scharnagl, N., Wischke, C., Sisson, A.L., Lendlein, A., 2012. Influence of co-monomer ratio on the chemical properties and cytotoxicity of poly[acrylonitrile-co-(N-vinylpyrrolidone)] nanoparticles. Journal of Applied Biomaterials & Functional Materials 10, 308-314.

Lucks, J.S., Müller, B.W., Müller, R.H., 1990. Polymeric and emulsion carriers—interaction with antiflocculants and ionic surfactants. International Journal of Pharmaceutics 63, 183-188.

Lundqvist, M., Sethson, I., Jonsson, B.-H., 2004. Protein Adsorption onto Silica Nanoparticles: Conformational Changes Depend on the Particles' Curvature and the Protein Stability. Langmuir 20, 10639-10647.

Lynch, I., Dawson, K.A., 2008. Protein-nanoparticle interactions. Nano Today 3, 40-47.

Maruthamuthu, M., Sobhana, M., 1979. Hydrophobic interactions in the binding of polyvinylpyrrolidone. Journal of Polymer Science: Polymer Chemistry Edition 17, 3159-3167.

Moghimi, S.M., 1997. Prolonging the circulation time and modifying the body distribution of intravenously injected polystyrene nanospheres by prior intravenous administration of poloxamine-908. A 'hepatic-blockade' event or manipulation of nanosphere surface in vivo? Biochimica et Biophysica Acta 1336, 1-6.

Moghimi, S.M., 2002. Chemical camouflage of nanospheres with a poorly reactive surface: towards development of stealth and target-specific nanocarriers. Biochimica et Biophysica Acta 1590, 131-139.

Moghimi, S.M., Muir, I.S., Illum, L., Davis, S.S., Kolb-Bachofen, V., 1993. Coating particles with a block co-polymer (poloxamine-908) suppresses opsonization but permits the activity of dysopsonins in the serum. Biochimica et Biophysica Acta 1179, 157-165.

Müller, R.H., 1997. Surface Hydrophobicity - Determination by ROSE Bengal (RB) Adsorption Methods, in: Müller, R.H., Mehnert, W. (Eds.), Particle and surface characterisation methods. Wissenschaftliche Verlagsgesellschaft, Stuttgart, pp. 215-228.

Müller, R.H., 1991. Colloidal carriers for controlled drug delivery and targeting - Modification, Characterization and in vivo Distribution. Wissenschaftliche Verlagsgesellschaft, CRC Press, Stuttgart, Germany; Boca Raton, USA.

Müller, R.H., Davis, S.S., Illum, L., Mak, E., 1986. Particle Charge and Surface Hydrophobicity of Colloidal Drug Carriers, in: Gregoriadis, G., Senior, J., Poste, G. (Eds.), Targeting of Drugs With Synthetic Systems. Springer US, pp. 239-263.

Müller, R.H., Heinemann, S., 1989. Surface Modelling of Microparticles as Parenteral Systems with High Tissue Affinity, in: Gurny, R., Junginger, H.E. (Eds.), Bioadhesion - Possibilities and Future Trends. Wissenschaftliche Verlagsgesellschaft, Stuttgart, pp. 202-214.

Müller, R.H., Lück, M., Kreuter, J., 2001. Medicament excipient particles for tissue specific application of a medicament. US Patent No.: 6288040B1.

Nagayama, S., Ogawara, K., Fukuoka, Y., Higaki, K., Kimura, T., 2007. Time-dependent changes in opsonin amount associated on nanoparticles alter their hepatic uptake characteristics. International Journal of Pharmaceutics 342, 215-221.

Ogawara, K., Furumoto, K., Nagayama, S., Minato, K., Higaki, K., Kai, T., Kimura, T., 2004. Pre-coating with serum albumin reduces receptor-mediated hepatic disposition of polystyrene nanosphere: implications for rational design of nanoparticles. Journal of Controlled Release 100, 451-455.

Paulke, B.-R., Möglich, P.-M., Knippel, E., Budde, A., Nitzsche, R., Müller, R.H., 1995. Electrophoretic 3D-mobility profiles of latex particles with different surface groups. Langmuir 11, 70-74.

Wan, L.S., Xu, Z.K., Huang, X.J., Wang, Z.G., Wang, H.L., 2005. Copolymerization of acrylonitrile with N-vinyl-2-pyrrolidone to improve the hemocompatibility of poly acrylonitrile. Polymer 46, 7715-7723.

Wei, Q., Becherer, T., Angioletti-Uberti, S., Dzubiella, J., Wischke, C., Neffe, A.T., Lendlein, A., Ballauff, M., Haag, R., 2014. Protein Interactions with Polymer Coatings and Biomaterials. Angewandte Chemie-International Edition 53, 8004-8031.

Wilkins, D.J., Myers, P.A., 1966. Studies on the relationship between the electrophoretic properties of colloids and their blood clearance and organ distribution in the rat. British Journal of Experimental Pathology 47, 568-576.

Wischke, C., Krüger, A., Roch, T., Pierce, B.F., Li, W., Jung, F., Lendlein, A., 2013. Endothelial cell response to (co)polymer nanoparticles depending on the inflammatory environment and comonomer ratio. European Journal of Pharmaceutics and Biopharmaceutics 84, 288-296.